UNIVERSIDAD NACIONAL DE COLOMBIA
SEDE MEDELLÍN
FACULTAD DE MINAS

DYNA
http://dyna.medellin.unal.edu.co/

Detection of open-pit mining zones by implementing spectral indices and image fusion techniques

Henry Omar A. Castellanos-Quiroz, Héctor Mauricio Ramírez-Daza & Yulia Ivanova

Center for Research and Development in Geographic Information CIAF –Agustín Codazzi Geographic Institute-IGAC, Group of Remote Sensing and Geographic Applications, Bogotá D.C., Colombia. henry.castellanos@igac.gov.co, hmramirez@igac.gov.co, yulia.ivanova@igac.gov.co.

Received: September 30th, 2016. Received in revised form: March 22th, 2017. Accepted: April 11th, 2017

Abstract
This article aims to present the results of the application of different proposed spectral indices and image fusion techniques for the detection of open-pit mining zones, located to the north-east of Antioquia, Colombia; having as reference mining and no mining zones samples obtained from visual characterization of pictorial-morphological properties of the open-pit mining zones in the study area. This research used high resolution (UltraCam-D y RapidEye) and medium resolution (Landsat 8 LDCM) imagery, where the latter was defined as the main input for the application of the spectral indices and image fusion techniques. The development of the proposed methodological design and the statistical analysis of the images, presented the Brovey transformed image fusion technique —on its band 2— as the one with the highest discriminant potential for open-pit mining zone; the classification of the results were determined between the thresholds of pixel values from 0.3225 —defined as the discriminant breakpoint— to the maximum value of the mining group samples, corresponding to 0.5237.

Keywords: Open-pit mining; spectral indices; images fusion; Fisher discriminant function analysis.

Detección de zonas mineras a cielo abierto aplicando índices espectrales y técnicas de fusión de imágenes

Resumen
Se presentan los resultados de la aplicación de diferentes índices espectrales y técnicas de fusión de imágenes de sensores remotos propuestos para la detección de zonas mineras a cielo abierto, localizadas en el sector nor-oriental del departamento de Antioquia, Colombia, tomando como referencia muestras de minería y no minería, identificadas a partir de la caracterización visual de propiedades pictoricomorfológicas de zonas mineras a cielo abierto en el área de estudio, utilizando imágenes de alta resolución (UltraCam-D y Rapid Eye) y mediana resolución (Landsat 8 LDCM), estas últimas fueron definidas como el insumo principal para la aplicación de los índices espectrales y técnicas de fusión de imágenes. El desarrollo del diseño metodológico propuesto y el análisis estadístico de las imágenes, evidenciaron que la técnica de fusión de imágenes, transformada de Brovey —en su banda 2— presenta mayor potencial discriminante para la identificación de zonas mineras a cielo abierto; la clasificación de los resultados se determinó entre el rango de valores de pixel de 0.3225 —constituido como el punto de corte discriminante— hasta el valor máximo de las muestras del grupo de minería, correspondiente a 0.5237.

Palabras clave: Minería a cielo abierto; índices espectrales; fusión de imágenes; relación discriminante Fisher.

1. Introduction

Currently in Colombia it is estimated that there are about 14,357 Units of Mining Production (UPM), of which 63% has no mining titles [1] and therefore are considered of an illegal character [2]. In the entire country at least 10 departments reported that over 80% of their UPM do not have any kind of mining title [1] which progressively makes more difficult their control, monitoring and their regulation regarding environment, as well as for labor, tax and legal aspects, causing disturbances in a national, regional and local context in social, economic, environmental, criminal, tax and

How to cite: A. Castellanos-Quiroz, H. O., Ramírez-Daza, H. M. and Ivanova, Y. Detección de zonas mineras a cielo abierto aplicando índices espectrales y técnicas de fusión de imágenes DYNA 84 (201) pp. 42-49, 2017.

public order issues, contrary to what aims the policy and legislative framework of Colombia. Because of this situation, it is necessary that the environmental and control authorities come to possess the technical and technological mechanisms of an official status that enables them to identify, monitor and report figures of areas of mining activity in the country, thus making it possible to efficiently and effectively fulfill their functions of control, monitoring and regulation.

In this sense, remote sensing products can be considered as a key tool in the detection and monitoring of different phenomena and dynamics on land cover, due to their characteristics and benefits in the provision of multispectral information. For this purpose there are different methodologies and specific applications that identify several features, such as different aspects related to the mining sector, where is included the use of remote sensing and geographic information systems on a wide array of issues like the identification of diverse minerals [3] the mapping of potential minerals like gold [4], the evaluation of mining impacts on land cover [5], illegal mining monitoring [6], studying the influence of mining on water quality [7,8], eco-toxicology of water in mining operations [9], environmental monitoring in areas of mining [10] and evaluating the subsidence caused by mining activities from image fusion techniques [11,12], among others.

However, few studies have shed light on processes specifically addressing the detection of open-pit mining zones, yet there are some investigations that contemplate approaches on this issue, some of them are associated with the identification of minerals presence for exploration stages [13], but not to operating areas or open-pit mining activity; in the aforementioned research they applied remote sensing in detecting alluvial gold in the Colombian Pacific Coast, based in the use of Landsat-TM and Spot-XS images as a fundamental instrument of exploration, and supported with geomorphological and field observations as ancillary information, they made use of individual bands analysis, spectral indices, and relationships between bands and filtering techniques, all this helped them identify extensions of palaeochannel, palaeovalley and flow deposits of mud genetically related to alluvial gold, i.e. new explorations banks.

Likewise, hyperspectral imaging has been used in detecting minerals [14] from the analysis of large amounts of spectral data, and as a result, the LinMin supervised classification algorithm was proposed to estimate the uncertainty of observed spectral information. Another interesting study has been developed for locating and identifying sites of gold mining in French Guiana [15], from the generation of spectral indices such as NDVI and NDWI, used as bands in a new image and with filters of contrast. Thus, it was possible the identification and classification of new ore mining areas.

Taking into account the need to availably have a methodology for the detection of open-pit mining areas, this study developed a procedure based on the application of spectral indices and image fusion techniques for the detection of open-pit mining process implemented in the north-eastern department of Antioquia, evaluating the accuracy of this methodology through statistical methods.

2. Study area

The study area is located in the northeastern sector of the department of Antioquia, Colombia, comprising sections of the municipalities of Nechí, Caucasia, Zaragoza and El Bagre, (7º 51' 1'' N, 74º 53' 34'' W y 74º 37' 15'' N, 7º 23' 58'' W) (Fig. 1), with an area of 150.000 ha. This has been traditionally an open-pit region which has had a recent increase in mineral production [16].

3. Materials and methods

As the main input for the application of spectral indices and image fusion techniques, data from the Landast 8 LDCM sensor dated June 17 of 2014 was used. Along with this data, high-resolution images as UltraCam-D and RapidEye were also used, which have been previously used to identify and characterize the pictorial-morphological properties[1] [17] of open-pit mining zones in the area under study [18]. The usage

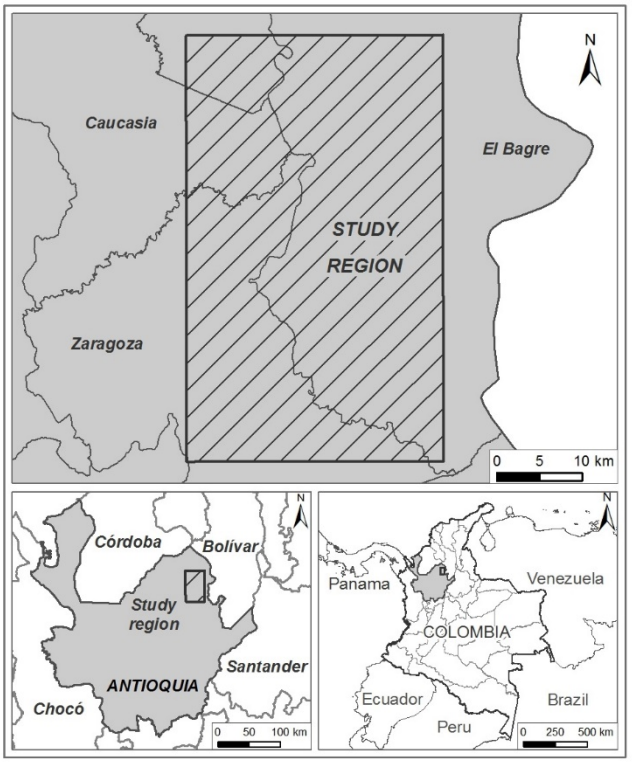

Figure 1. Location of the region under study.
Source: The Authors.

[1]Pictorial-morphological characteristics are the elements in the image that allow or serve as concurrent evidence for the identification of objects and their differentiation from other coverages [17] pictorial features are also known as morphological descriptors [19] or visual interpretation criteria [20]. Among such pictorial-morphological characteristics, the analysis of shape, size, color, tone, texture, pattern and geographical position [21] are used comprehensively in complex visual classifications.

of the aforementioned data allowed the visual definition, differentiation and delimitation of mining areas from non-mining areas.

For the methodology of this study, nine spectral indices and two image fusion techniques were proposed and implemented for the detection of open-pit mining zones (Table 1), defined from reviewing previous specialized literature, where some of these indices and fusion techniques were designed and/or commonly implemented for the detection and the analysis of eroded zones [22], detection of minerals, soil types and/or rocks [23,24].

For each spectral index and image fusion technique, data of Mining and Non-Mining (which are the defined thematic classes of the study) was obtained by selecting trough the samples taken directly from the Landsat 8 LDCM image (some of which are shown in Fig. 2) image. For the samples of the thematic class "Mining", these were made from the identification and characterization of its pictorial-morphological properties obtained through visual interpretation [18], both from the high resolution images (Ultra CAMD) as from the medium resolution ones (LDCM Landsat 8). As for the thematic class "No Mining", the procedure consisted in the application of the Normalized Difference Vegetation Index (NDVI) in order to exclude coverage of photosynthetically active vegetation, where the inexistence of open-pit mining is manifest. From this result the samples were selected for the thematic class of No Mining, which mainly includes coverage of eroded areas, rocky areas, population centers and clean pastures (Fig. 2).

Table 1.
Spectral indices and image fusion techniques

Name	Abbreviation	Equation	Source
Clay minerals	CM	SWIR1 / SWIR2	[23]
Ferrous minerals	FM	SWIR1 / NIR	[23, 24]
Iron oxide (ferric minerals)	IO	RED / BLUE	[23, 24]
Transformed normalized difference vegetation index	TNDVI	SQRT ((NIR – RED / NIR + RED) + 0,5)	[25, 26]
Normalized difference vegetation index	NDVI	NIR – RED / NIR + RED	[27]
Difference vegetation index	DVI	NIR – RED	[28]
Simple ratio	SR IR/R	NIR / RED	[28]
SQRT simple ratio	SQRT SR IR/R	SQRT (NIR / RED)	[26]
Principal components	CP	Function Erdas Imagine© 2011	[29]
Fusion Brovey	Brovey	BAND_OUT = BAND / [(BLUE + GREEN + RED) x PAN].	[30]
Fusion Wavelet	Wavelet	Function Erdas Imagine© 2011	[31]

NIR = near infrared spectrum, RED= red spectrum, SWIR = short wave infrared spectrum, BLUE= blue spectrum, GREEN= green spectrum, PAN = pancromatic.
Source: The Authors.

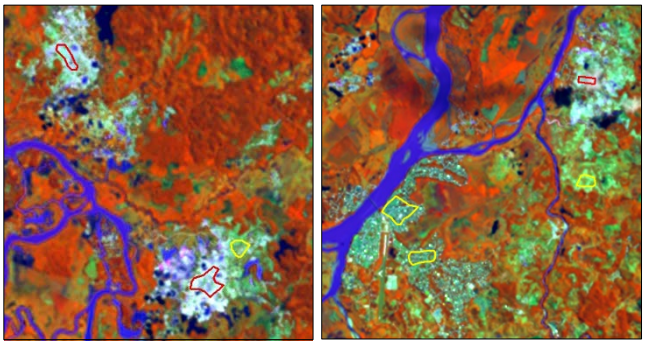

Figure 2. Samples of the thematic classes of Mining (red polygons) and Non-Mining (yellow polygons). Image Landsat 8 LDCM 955 20140617, RGB (5, 6, 4), USGS.
Source: The Authors.

From these samples, 515 observations were obtained for Mining and 461 for Non-Mining to the application of spectral indices, whereas for the image fusion technique, 1.985 were for Mining and 1.883 for No Mining, both these set of samples correspond to the same sampled area (polygons), the more data for image fusion techniques is due to the fact that higher spatial resolution images are used.

In order to obtain the spectral index or image fusion technique with the highest potential for discriminating mining from non-mining areas, the Fisher's discriminant ratio (or Fisher's index) was used. This index allows obtaining a series of linear functions (discriminant functions) through the independent variables that assists in the interpretation of differences between various groups. This technique is widely used in spatial analysis to quantify the degree of separability of individual characteristics [32] based on statistical parameters of the mean ($\boldsymbol{\mu}$) and the variance ($\boldsymbol{\sigma}$) [33]. In the case of multiple classes Fisher's index is expressed by Eq. 1:

$$FDR = \sum_{i}^{M} \sum_{j \neq i}^{M} \frac{(\mu_i - \mu_j)^2}{{\sigma_i}^2 + {\sigma_j}^2} \quad (1)$$

Where μ_i and σ_i refer to the corresponding mean and variance values of the Mining areas samples characteristics, μ_j and σ_j, are the mean and variance values of the Non-Mining areas. The characteristics with the highest Fisher's ratio are more discriminating than those with lower index [33].

The Fisher's separability criterion applies to samples that respond to various conditions. First, samples should have statistically different mean values; this condition is verified through the Student criterion [34]. Second, the two classes must follow a normal probability distribution; this condition is verified through the construction of empirical and normal probability curves for each class, and the subsequent demonstration of the goodness of fit between the two curves using the criteria of Kolmogorov-Smirnov test and $\boldsymbol{\chi^2}$ [35]. All the analyses were performed to the

level of two-tailed significance test $2\alpha = 5\%$ for each class.

By fulfilling all the conditions listed above, the index with the best separation potential of mining from non-mining areas can now be selected, according to the highest value of Fisher's index.

In order to be able to tell a mining from a non-mining region apart using the pixel value, the discriminant breakpoint was used. This is estimated as the average of the two-groups pixel value average, as expressed in Eq. 2:

$$PCD = \frac{\mu_i + \mu_j}{2} \quad (2)$$

where:

PCD : Discriminant breakpoint
μ_i : The average value of the pixel from the mining area sample
μ_j : The average value of the pixel from the non-mining area sample

To evaluate the classification rule the apparent error rate equation is used, which is expressed as follows:

$$RAE = \frac{Wrongly\ classified\ data}{Sample\ size} \times 100\% \quad (3)$$

where:

RAE : Apparent error rate
$Wrongly\ classified\ data$: Number of the sample data that are outside the range stipulated by the discriminant breakpoint
$Sample\ size$: Total number of data (pixels)

The apparent error rate was calculated for both samples of mining and non-mining areas. Afterwards, the weighted average value that characterized the weighted rate of the apparent error was obtained.

4. Results and discussion

Initially, the level of separation of mining and non-mining classes for every spectral indices and image fusion techniques applied was visually evaluated from the comparative analysis of histograms.

This analysis is based on the degree of separability between the histograms of the samples in each of the spectral indices and images fusion techniques discussed, where the greater the distance or separation between histograms, the greater it's potential to discriminate mining from non-mining areas; likewise, the lower the shared area between histograms, the greater the discriminant potential of the spectral index and image fusion technique. The shared area between histograms determines the inaccuracy of the discriminant power of the index or of the technique employed.

Figs. 3 and 4 shows the comparison of histograms for the nine spectral indices and for the two image fusion techniques employed. These figures illustrate that both the iron oxide spectral index (Fig. 3c), as the band 2 of the Brovey transform technique (Fig. 4b), have better degrees of separability and less shared area between histograms (the greater distance between the histograms peaks, the better the discriminant power). This shows a better potential to classify mining from non-mining areas compared to other indices and fusion techniques. Likewise, the indices and fusion techniques analyses allowed an evaluation of areas with less potential for mining areas, including the spectral indices of clay minerals (Fig. 3a) and ferrous minerals (Fig. 3b).

Subsequently, Fisher's index was used to statistically evaluate the discriminant power of the nine spectral indices, and the six bands resulting of the two image fusion techniques. The implementation of this index is subject, as previously mentioned, to compliance with the conditions that the two samples present a normal distribution and that their average values are statistically different.

Fisher's index is calculated once these conditions are met, and after analyzing the results it was found that the best image fusion technique was the Brovey transform in his band 2, since this technique had the highest Fisher's index value. Therefore, this is established as the technique with the highest discriminant power to classify mining from non-mining areas. Fisher's index results for each of the techniques are presented in Table 2.

As it has been mentioned, the concept of discriminant breakpoint was used for the definition of the pixel's value that separates the mining from non-mining class, which represents the average value between the two classes. Since the data of these two classes follow a normal distribution, the modal value corresponds to the value of the arithmetic mean (Eq. 2). The resulting value of the discriminant point is 0.3225; therefore, every pixel with a value under 0.3225 was associated with the class of non-mining and values between 0.3225 and, the maximum value of for the mining class of 0.5237 (Table 2), correspond to the classification of mining.

To evaluate the validity of this classification scheme, the apparent error rate for the two classes was calculated and used to estimate the weighted apparent error rate, taking into account the amount of data in each class, according to Eq.3.

For the mining class, there were a total of 1.985 records where 223 of them were outside the range according to the value of the discriminant point, thus— resulting in apparent error rate of 11.2%. As for the non-mining class, it consisted of 1.883 records, 118 of which did not belong to the range set by the value of the discriminant point. The value of the apparent error rate is 6.4% and the weighted value of the apparent error rate corresponds to 8.9%.

Fig. 5 shows an example of the results obtained from the classification of open-pit mining zones using the Brovey transform in its band 2:

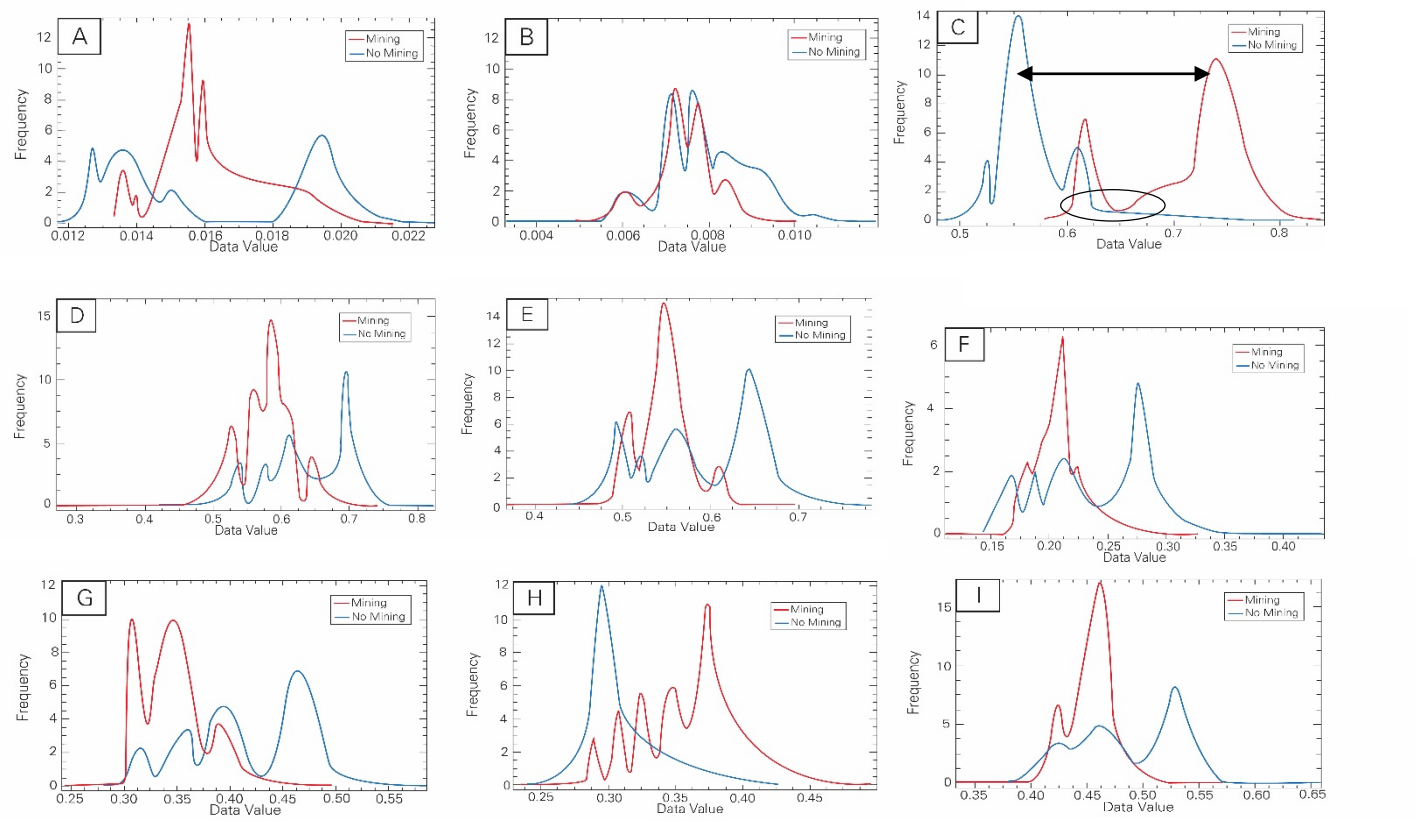

Figure 3. Histograms comparison of the spectral indices for mining and non-mining classes.
Spectral indices: a = clay minerals, b = ferrous minerals, c = iron oxide (ferric minerals), d = TNDVI, e = NDVI, f = simple ratio, g = DVI, h = principal components, i = sqrt simple ratio.
Source: The Authors.

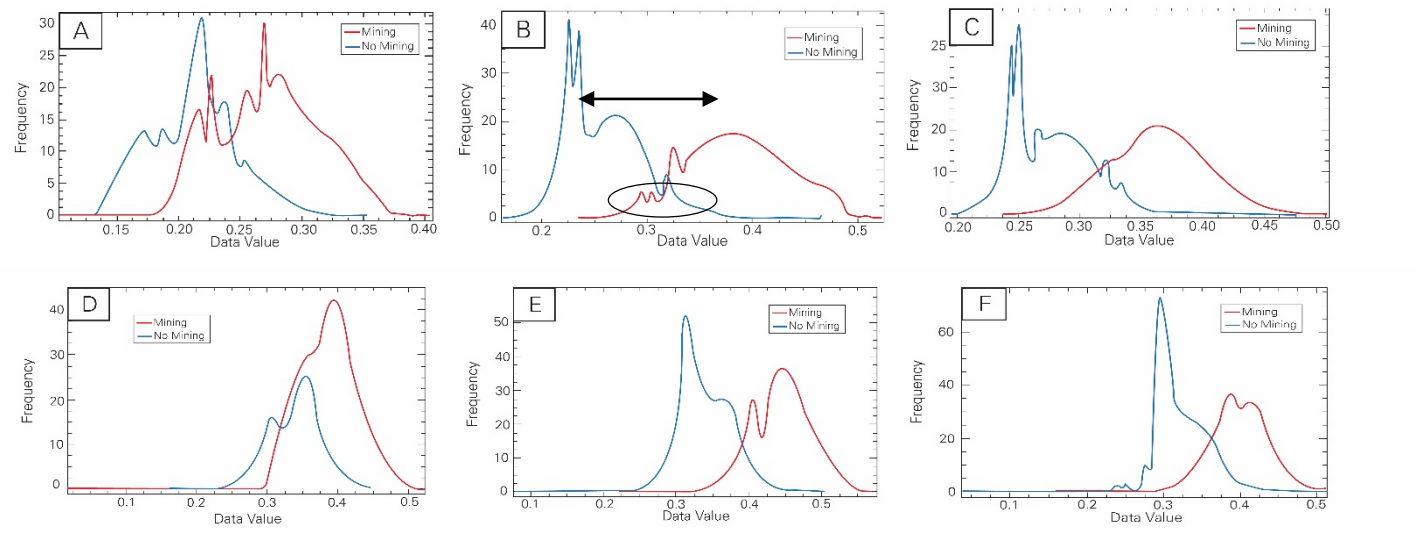

Figure 4. Histograms comparison of the images fusion techniques for mining and non-mining classes.
Image fusion techniques: Brovey fusion a = band1, b = band2, c = band3. Wavelet fusion d = band1, e = band2, f = band3.
Source: The Authors.

Table 2.
Discriminant power values according to Fisher's ratio.

Spectral indices and image fusion techniques	Mining				Non Mining				
	Min.	Max.	Media	SD*	Min.	Max.	Media	SD*	FDR**
Clay Minerals	0,01333	0,02267	0,01647	0,00166	0,01167	0,02273	0,0166	0,00304	0,00000
Ferrous Minerals	0,00466	0,01007	0,00747	0,00078	0,00327	0,01192	0,00805	0,00118	0,00016
Iron Oxide	0,57771	0,84079	0,71605	0,05637	0,47798	0,81561	0,58242	0,05575	0,15927
TNDVI	0,27116	0,74425	0,58109	0,04328	0,41978	0,82502	0,62909	0,07541	0,01940
NDVI	0,36789	0,69564	0,54938	0,03400	0,43795	0,78213	0,59161	0,06366	0,01825
Simple Ratio IR/R	0,11080	0,32847	0,20803	0,02324	0,14296	0,43445	0,24116	0,04851	0,01530
DVI	0,24145	0,52038	0,34963	0,03666	0,28868	0,58669	0,41494	0,05788	0,04512
Principal Components	0,22944	0,49949	0,37474	0,04886	0,23874	0,42861	0,30858	0,02990	0,05557
SQRT Simple Ratio	0,33287	0,57312	0,45541	0,02509	0,37810	0,65912	0,48861	0,04930	0,01480
Fusion Brovey b1	0,102632	0,405798	0,276628	0,043670	0,129313	0,352955	0,215832	0,038883	0,044773
Fusion Brovey b2	0,23399	0,52370	0,38782	0,04966	0,16153	0,46510	0,26448	0,04159	0,16669
Fusion Brovey b3	0,23680	0,50283	0,36759	0,04199	0,19373	0,47682	0,27829	0,03663	0,10140
Fusion Wavelet b1	0,01816	0,52410	0,38967	0,04094	0,16098	0,44768	0,33866	0,03893	0,03257
Fusion Wavelet b2	0,15785	0,57595	0,44899	0,04255	0,07567	0,50531	0,34262	0,03853	0,13955
Fusion Wavelet b3	0,11004	0,51312	0,40129	0,03783	0,03641	0,50656	0,32582	0,03547	0,07769

*SD: Standard deviation. **FDR: Fisher's discriminant ratio.
Source: The Authors.

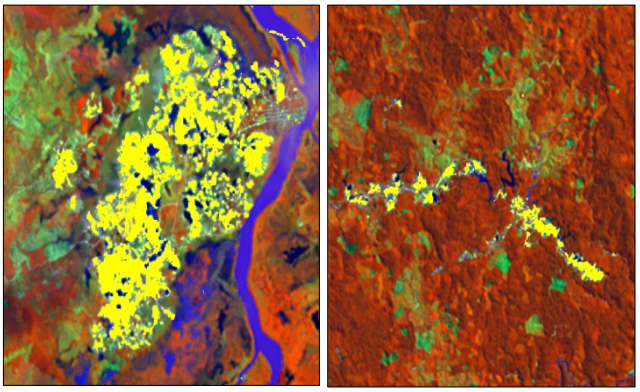

Figure 5. Classification of open-pit mining zones in the study area (yellow polygons), using the Brovey transform in its band 2.
Source: The Authors.

5. Conclusions and recommendations

The Brovey transform image fusion technique in its band 2 was determined as the procedure with the highest discriminant power to classify open-pit mining zones, using as classification thresholds values between 0.3225 and 0.5237 for the area under study, with a weighted apparent error rate of 8.9%. It is important to highlight however, that this value is conditioned by the size of the mining and non-mining samples.

It was also shown that the ferrous minerals and clay minerals spectral indices have the least discriminant power for the area under study, despite the fact that these indices have been mainly designed for, and implemented in, the detection of certain types of minerals.

From the results obtained, the Brovey transform image fusion technique is identified as a major input for the detection and identification of open-pit mining areas, with a plausible prospection of being used as part of a monitoring system for such areas.

It is recommended to incorporate to the results presented in this article, an object-oriented image analysis, which enables the integration of other elements that could lead to the constitution of a new mappable thematic unity of the official map of land cover (Corine Land cover) called "Mining Zones".

Acknowledgements

We want to give our most profound thanks to the whole team of Remote Sensing and Geographic Applications of the Research and Development Center for Geographic Information (CIAF), Instituto Geográfico Agustín Codazzi (IGAC), especially to Nelson Nieto, Andrés Espejo and Luz Ángela Uscategui for their valuable technical and scientific contribution.

References

[1] Ministerio de Minas y Energía (MME), República de Colombia. Censo minero departamental colombiano 2010-2011. Bogotá D.C.: MME, [en línea]. 2012. [date of reference May 5th of 2016]. Available at: https://www.minminas.gov.co/censominero.

[2] Ministerio de Minas y Energía (MME), República de Colombia. Glosario técnico minero. [en línea]. Bogotá D.C.: MME, 2015 [date of reference May 5th of 2016]. Available at: http://www.minminas.gov.co/glosario-minero1.

[3] King, T.V.V., Johnson, M.R., Hubbard, B.E. and Drenth, B.J. (Eds.). Identification of mineral resources in Afghanistan-Detecting and mapping resource anomalies in prioritized areas using geophysical and remote sensing (ASTER and HyMap) data. U.S. Geological Survey Open-File Report [online]. 2011-1229, 2011, 327 P. Available at: http://pubs.usgs.gov/of/2011/1229/.

[4] Kwang, C., Osei, E.M. and Duker, A.A., Application of remote sensing and geographic information systems for gold potential mapping in Birim north district of Eastern Region of Ghana - Gold potential mapping using GIS and remote sensing. International Journal of Remote Sensing Applications, 4(1), pp. 48-55, 2014. DOI: 10.14355/ijrsa.2014.0401.05.

[5] Glenn, B., Prakash, A. and Sokol, E., Coal and peat fires: A global perspective. [online].Vol. 3: Case Studies – Coal Fires, Chapter 9, Impact of mining activities on land use land cover in the Jharia Coalfield, India, pp. 263-279, 2015. [date of reference May 5th of 2016], Available at http://linkinghub.elsevier.com/retrieve/pii/B9780444595096000090.

[6] Ji, M., Li, X., Wu, S., Gao, Y. and Ge, L., Use of SAR interferometry for monitoring illegal mining activities: A case study at Xishimen iron ore mine. International Journal of Mining Science and Technology, 21(6), pp. 781-786, 2011. DOI: 10.1016/j.mstc.2011.05.039.

[7] Doña, C., Chang, N., Caselles, V., Sánchez, J., Camacho, A., Delegido, J. and Vannah, B., Integrated satellite data fusion and mining for monitoring lake water quality status of the Albufera de Valencia in Spain. Journal of Environmental Management 151, pp. 416-426, 2015. DOI: 10.1016/j.jenvman.2014.12.003.

[8] Ribeiro, L., Kretschmer, N., Nascimento, J., Buxo, A., Rötting, T.S., Soto, G., Soto, M., Oyarzún, J. Maturana, H. and Oyarzún, R., Water quality assessment of the mining-impacted Elqui River Basin, Chile. Mine Water and the Environment, 33(2), pp. 165-176, 2014. DOI: 10.1007/s10230-014-0276-6.

[9] Harford, A., Hogan, A., Jones, D. and Van Dam, R., Ecotoxicology of highly treated mine waters: Lessons from an Australian mine. Mine Water and the Environment, [online]. 34(1), pp. 75-86, 2015. Available at: http://link.springer.com/10.1007/s10230-014-0282-8.

[10] Yang, L. and Jiuyun, S., Study of the integrated environmental monitoring in mining area based on image analysis. Procedia Engineering, 21, pp. 267-272, 2011. DOI: 10.1016/j.proeng.2011.11.2014.

[11] Wang, X., Wang, Y. and Huang, T., Extracting mining subsidence land from remote sensing images based on domain knowledge. Journal of China University of Mining and Technology. 18(2), pp. 168-181, 2008.

[12] Li, L.J. and Wu, Y.B., Application of remote-sensing-image fusion to the monitoring of mining induced subsidence. Journal of China University of Mining and Technology, 18(4), pp. 531-536, 2008.

[13] Forero, H., Lopez, J. y McCourt, W., Aplicación de los sensores remotos en la detección de aluviones auríferos en la costa pacífica colombiana. Simposio Internacional sobre yacimientos aluviales de oro, La Paz, Bolivia, 1-5 de junio de 1991. [en línea]. Disponible en: http://horizon.documentation.ird.fr/exl-doc/pleins_textes/pleins_textes_6/colloques2/36212.pdf.

[14] Schmidt, F., Legendre, M. and Le Mouëlic, S., Minerals detection for hyperspectral images using adapted linear unmixing: LinMin. Icarus 237, pp. 61-74, 2014. DOI: 10.1016/j.icarus.2014.03.044.

[15] Gond, V. and Brognoli, C., Télédétection et aménagement du territoire: localisation et identification des sites d'orpaillage en Guyane française. Bois et Forêts des Tropique, [online]. 286(4), pp. 5-13, 2005. Available at: https://agritrop.cirad.fr/528994/1/document_528994.pdf.

[16] Ministerio de Minas y Energía (MME), República de Colombia. Producción y exportaciones de metales preciosos en Colombia 2013. Bogotá D.C.: MME, 2014 [consultado el 5 de mayo de 2016]. Available at: http://www.minminas.gov.co/analisis-minero.

[17] Melo, L. y Camacho, M., Interpretación visual de imágenes de sensores remotos y su aplicación en levantamientos de coberturas y uso de la Tierra. Bogotá: IGAC, 2005.

[18] Castellanos, H.O., Espejo, A. y Ramírez, M., Diseño metodológico para la identificación y monitoreo de zonas mineras en Colombia a partir de sensores remotos. Centro de Investigación y Desarrollo en Información Geográfica (CIAF), Grupo de Percepción Remota y Aplicaciones Geográficas del Instituto Geográfico Agustín Codazzi (IGAC). Bogotá D.C., 2015.

[19] Lira, J., Tratamiento digital de imágenes multiespectrales. México D.F.: Universidad Nacional Autónoma de México, 2010.

[20] Chuvieco, E., Teledetección ambiental. Nueva edición actualizada. Madrid: Ariel Ciencia, 2010.

[21] Li, N., Yan, C.Z. and Xie, J.L., Remote sensing monitoring recent rapid increase of coal mining activity of an important energy base in northern China, a case study of Mu Us sandy land. Resources, Conservation and Recycling 94, pp. 129-135, 2015. DOI: 10.1016/j.resconrec.2014.11.010.

[22] Otero, J., Sánchez, R., Ojeda, E., Álvarez, C., Gómez, C., Carrillo, H., Castro, C., Palacios, A. y Camacho, M., Protocolo para la identificación y evaluación de los procesos de degradación de suelos y tierras por erosión. Bogotá D.C.: MVDT, IGAC e IDEAM, [en línea]. 2012. Available at: http://www.ideam.gov.co/documents/11769/241818/20120814_Protocolo_desertificacion.pdf/c34ac460-215b-4cb8-8ffe-a8f9218e2bac.

[23] Drury S., A. image interpretation in geology. London: Allen & Unwin, 1987.

[24] Segal D., Theoretical basis for differentiation of ferric-iron bearing minerals, using landsat MSS data. Proceedings of Symposium for Remote Sensing of Environment, 2nd Thematic Conference on Remote Sensing for Exploratory Geology, Fort Worth, TX., 1982. pp. 949-951.

[25] Rouse, J.W., Monitoring the vernal advancement and retrogradation green wave effect of natural vegetation. Texas: Remoting Sensing Center, 1973.

[26] Sebem, E., Aportaciones de la teledetección en el desarrollo de un sistema metodológico para la evaluación de los efectos del cambio climático sobe la producción de las explotaciones agrarias. Tesis Dr., Departamento de Ingeniería Cartográfica, Geodesia y Fotogrametría. Universidad Politécnica de Madrid, Madrid, España, 2005.

[27] Kriegler, F., Malila, W.A., Nalepka, R.F. and Richardson, W., Preprocessing transformations and their effects on multispectral recognition. Proceedings of the Sixth International Symposium on Remote Sensing of Environment, Ann Arbor, MI, USA, 13-16 October, 1969. pp. 97-131.

[28] Tucker C.J., Red and photographic infrared linear combinations for monitoring vegetation. Remote Sensing of Environment, 8(2), pp. 127-150, 1979.

[29] López, J.F., Fernández, S. y Lozada, C., Análisis factorial con componentes principales para interpretación de imágenes satelitales "Landsat TM 7" aplicado en una ventana del departamento de Risaralda. Scientia et Technica, 1(38), pp. 241-246, 2008.

[30] Earth Resource Mapping Pty Ltd. The Brovey Transform Explained. EMU Forum, 2(11), 1990.

[31] Nunez, J., Otazu, X., Fors, O., Prades, A., Pala, V. and Arbiol, R., Multiresolution-based image fusion with additive wavelet decomposition. IEEE Transactions on Geoscience and Remote Sensing, 37(3), pp. 1204-1211, 1999. DOI: 10.1109/36.763274.

[32] Sandoval, Z. y Prieto, F., Caracterización de café cereza empleando técnicas de visión artificial. Revista Facultad Nacional de Agronomía, [en línea]. 60(2), pp. 4105-4127, 2007. Disponible en: http://www.scielo.org.co/scielo.php?script=sci_arttext&pid=S0304-28472007000200015.

[33] Ariza, A., García, S. Rojas, S. y Ramírez, M., Desarrollo de un modelo de corrección de imágenes de satélite para inundaciones: (CAIN - Corrección Atmosférica e Índices de Inundación). [en línea]. Bogotá D.C.: Centro de Investigación y Desarrollo en información Geográfica del IGAC-CIAF, UN-SPIDER Regional Support Office in Colombia, 2014. Disponible en: http://docplayer.es/2900781-Desarrollo-de-un-modelo-de-correccion-de-imagenes-de-satelite-para-inundaciones-cain-correccion-atmosferica-e-indices-de-inundacion.html.

[34] Peña, D., Fundamentos de estadística. Madrid: Alianza Editorial, 2008.

[35] Ortuño, M.T. and Sanz, L., Cálculo de probabilidades. Madrid: Anaya, 2006.

H.O.A. Castellanos-Quiroz, is BSc. in Forestal Eng. of the Industrial University of Santander, Colombia, MSc. in Geomatics of the Universidad Nacional de Colombia. He is research associate at the Center for Research and Development in Geographic Information (CIAF) of the Agustín Codazzi Geographic Institute (IGAC), Group of Remote Sensing and Geographic Applications. Bogotá, Colombia.
ORCID: 0000-0002-9673-2681

H.M. Ramírez-Dáza, is BSc. in Forestal Eng. of the Francisco José de Caldas Distrital University, Colombia, MSc. in Geography of Politecnical and Technological University of Tunja, Colombia. Head of the Center for Research and Development in Geographic Information (CIAF) of the Agustín Codazzi Geographic Institute (IGAC).
ORCID: 0000-0002-1672-4076

Y. Ivanova, is BSc. in Hidrology Eng. of the Limnological Institute of Russian Academy of Sciences, Russia. MSc. in Environmental Management of the Pontificia Javeriana University, Colombia. She is research associate at the Center for Research and Development in Geographic Information (CIAF) of the Agustín Codazzi Geographic Institute (IGAC), Group of Remote Sensing and Geographic Applications. Bogotá, Colombia.
Orcid: 0000-0001-8836-5175